

Adaptive spatial-temporal detection of multiple moving objects in subcellular time-lapse assays

Samuel V. Alworth¹, Seho Oh¹, Tuan Phan¹, Duk-Su Koh³, Wendy E. Thomas², James SJ Lee¹

¹SVision LLC, 3633 136th Pl. SE, Suite 300, Bellevue, WA 98006, USA

²Department of Bioengineering, University of Washington, Seattle, WA

³Department of Physiology & Biophysics, University of Washington, Seattle, WA



Introduction

A new generation of microscope and fluorescent probe technologies is enabling the quantitative characterization of the dynamics of discrete proteins and organelles in living cells. Assays using time-lapse images are now common, yet the state of the art image informatics tools use outdated detection and tracking technologies. Consequently, quantitative kinetic analysis of such data is largely manual; which is tedious, time consuming and subjective.

We developed an adaptive spatial-temporal algorithm for the simultaneous detection of multiple moving objects in a highly automated fashion even when they are difficult to distinguish from each other and/or from background. Our goal is to create a robust detection method, used by a generic tracking approach that can ultimately be applied to a broad range of particle tracking assays (see our other poster LB7).

The detection algorithm applies adaptive processing to generate a confidence map of tracking match candidates. The candidates are connected across frames using a matching step to create tracks. In this study, we have compared standard correlation based track candidate matching with our new spatial-temporal method using two sets of time-lapse images from vesicle tracking experiments. The methods are evaluated by comparing their overall tracking accuracy while holding other tracking algorithm elements constant. The tracking "truth" was created manually and validated by independent review and correction. The results show clearly that the spatial-temporal matching is superior to correlation based matching for these experiments.

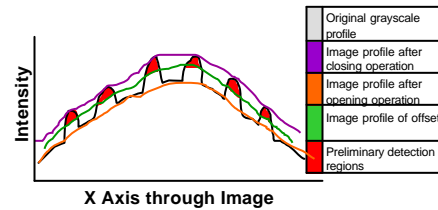


Fig 2. Adaptive processing generates high confidence detection regions by applying grayscale morphological image processing operations. Morphology based region detection does not introduce phase shift or blurring effect. In adaptive processing, the confidence map containing detection regions is produced by A) Applying grayscale morphological closing to the input image to generate the closed image, B) Applying grayscale morphological opening to the input image to generate the opened image, C) generating the offset image by subtracting the closed image from the opened image and adding an offset, and D) subtracting the offset image from the original image.

Adaptive spatial-temporal detection

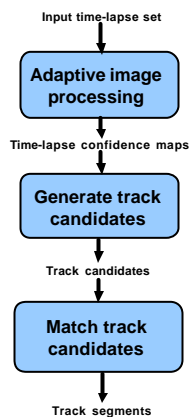


Fig 1. Adaptive spatial temporal detection consists of three steps. Input time-lapse images are adaptively processed to generate confidence maps. The high confidence map regions are then detected. The morphology of the detection regions is considered to produce track candidates. Future and past positions of track candidates are then considered to match objects into track segments.

An alternative approach was evaluated using a standard correlation method applied to the confidence maps directly to find track candidates, and thereby avoiding the adaptive spatial-temporal detection, checking and matching.

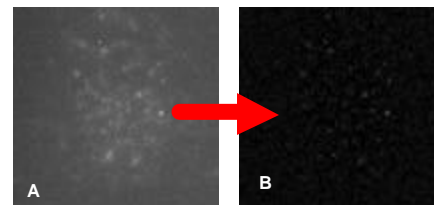


Fig 3. Adaptive processing creates high confidence detection regions called "confidence maps". (A) shows a representative image frame from one of the study time-lapse series containing vesicles of interest. (B) shows the confidence map produced through adaptive processing. In the confidence map, high pixel values correspond to higher confidence that the pixel belongs to an object of interest, and is thus a good tracking candidate. In the correlation method, tracking candidates are matched directly in the confidence maps.

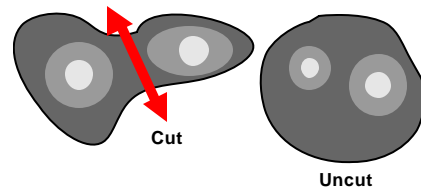


Fig 4. Morphology of high confidence regions are considered to generate final tracking match candidates. If there are multiple peaks within a confidence detection region, the region is cut into two candidates only if the region has a non circular shape. In this figure, regions of non zero confidence are shown, where the brighter regions are higher confidence peaks.

$$S_{match} = e^{-R_{conf}/2} \quad P_{match} = \begin{cases} \frac{V_{c1}^2}{a} = I_{conf} & \dots \dots \dots \text{if } (V_c^2 = 0) \\ \frac{(V_{c1} \bullet V_c - V_c^2)^2}{V_c^2(a + V_c^2 + b)} & \frac{V_{c2}^2 \bullet V_c^2 - (V_{c1} \bullet V_c)^2}{a + V_c^2 + d + (V_{c1} \bullet V_c)^2} & \dots \dots \dots \text{else} \end{cases}$$

in which a is a constant $b = \frac{c_1 \bullet F^2}{c_2 \bullet F^2}$ $c_1 = \frac{1}{2} \bullet \frac{V_{c1}^2 + V_c^2 - (V_c \bullet V_c)^2}{(V_c \bullet V_c)^2}$ $c_2 = \frac{1}{2} \bullet \frac{V_{c2}^2 + V_c^2 - (V_c \bullet V_c)^2}{(V_c \bullet V_c)^2}$ $F = \frac{I_{conf}}{I_{max}}$ I_{conf} : top 10% intensity level of the object in the confidence map I_{max} : the maximum real intensity of the object at $n+1$ frame.

and $\Delta t_{c1} = x_{c1} - x_c$ $\Delta t_{c2} = y_{c1} - y_c$ $\Delta t_{c3} = z_{c1} - z_c$ $\Delta t_{c4} = x_{c2} - x_c$ $\Delta t_{c5} = y_{c2} - y_c$ $\Delta t_{c6} = z_{c2} - z_c$ $\Delta t_{c7} = \frac{I_{c1} - I_{c2}}{I_{c1} + I_{c2}}$ $\Delta t_{c8} = \frac{I_{c1} - I_{c2}}{I_{c1} + I_{c2}}$ $\Delta t_{c9} = \frac{I_{c1} - I_{c2}}{I_{c1} + I_{c2}}$ $\Delta t_{c10} = \frac{I_{c1} - I_{c2}}{I_{c1} + I_{c2}}$ $\Delta t_{c11} = \frac{I_{c1} - I_{c2}}{I_{c1} + I_{c2}}$ $\Delta t_{c12} = \frac{I_{c1} - I_{c2}}{I_{c1} + I_{c2}}$ $\Delta t_{c13} = \frac{I_{c1} - I_{c2}}{I_{c1} + I_{c2}}$ $\Delta t_{c14} = \frac{I_{c1} - I_{c2}}{I_{c1} + I_{c2}}$ $\Delta t_{c15} = \frac{I_{c1} - I_{c2}}{I_{c1} + I_{c2}}$ $\Delta t_{c16} = \frac{I_{c1} - I_{c2}}{I_{c1} + I_{c2}}$ $\Delta t_{c17} = \frac{I_{c1} - I_{c2}}{I_{c1} + I_{c2}}$ $\Delta t_{c18} = \frac{I_{c1} - I_{c2}}{I_{c1} + I_{c2}}$ $\Delta t_{c19} = \frac{I_{c1} - I_{c2}}{I_{c1} + I_{c2}}$ $\Delta t_{c20} = \frac{I_{c1} - I_{c2}}{I_{c1} + I_{c2}}$ $\Delta t_{c21} = \frac{I_{c1} - I_{c2}}{I_{c1} + I_{c2}}$ $\Delta t_{c22} = \frac{I_{c1} - I_{c2}}{I_{c1} + I_{c2}}$ $\Delta t_{c23} = \frac{I_{c1} - I_{c2}}{I_{c1} + I_{c2}}$ $\Delta t_{c24} = \frac{I_{c1} - I_{c2}}{I_{c1} + I_{c2}}$ $\Delta t_{c25} = \frac{I_{c1} - I_{c2}}{I_{c1} + I_{c2}}$ $\Delta t_{c26} = \frac{I_{c1} - I_{c2}}{I_{c1} + I_{c2}}$ $\Delta t_{c27} = \frac{I_{c1} - I_{c2}}{I_{c1} + I_{c2}}$ $\Delta t_{c28} = \frac{I_{c1} - I_{c2}}{I_{c1} + I_{c2}}$ $\Delta t_{c29} = \frac{I_{c1} - I_{c2}}{I_{c1} + I_{c2}}$ $\Delta t_{c30} = \frac{I_{c1} - I_{c2}}{I_{c1} + I_{c2}}$ $\Delta t_{c31} = \frac{I_{c1} - I_{c2}}{I_{c1} + I_{c2}}$ $\Delta t_{c32} = \frac{I_{c1} - I_{c2}}{I_{c1} + I_{c2}}$ $\Delta t_{c33} = \frac{I_{c1} - I_{c2}}{I_{c1} + I_{c2}}$ $\Delta t_{c34} = \frac{I_{c1} - I_{c2}}{I_{c1} + I_{c2}}$ $\Delta t_{c35} = \frac{I_{c1} - I_{c2}}{I_{c1} + I_{c2}}$ $\Delta t_{c36} = \frac{I_{c1} - I_{c2}}{I_{c1} + I_{c2}}$ $\Delta t_{c37} = \frac{I_{c1} - I_{c2}}{I_{c1} + I_{c2}}$ $\Delta t_{c38} = \frac{I_{c1} - I_{c2}}{I_{c1} + I_{c2}}$ $\Delta t_{c39} = \frac{I_{c1} - I_{c2}}{I_{c1} + I_{c2}}$ $\Delta t_{c40} = \frac{I_{c1} - I_{c2}}{I_{c1} + I_{c2}}$ $\Delta t_{c41} = \frac{I_{c1} - I_{c2}}{I_{c1} + I_{c2}}$ $\Delta t_{c42} = \frac{I_{c1} - I_{c2}}{I_{c1} + I_{c2}}$ $\Delta t_{c43} = \frac{I_{c1} - I_{c2}}{I_{c1} + I_{c2}}$ $\Delta t_{c44} = \frac{I_{c1} - I_{c2}}{I_{c1} + I_{c2}}$ $\Delta t_{c45} = \frac{I_{c1} - I_{c2}}{I_{c1} + I_{c2}}$ $\Delta t_{c46} = \frac{I_{c1} - I_{c2}}{I_{c1} + I_{c2}}$ $\Delta t_{c47} = \frac{I_{c1} - I_{c2}}{I_{c1} + I_{c2}}$ $\Delta t_{c48} = \frac{I_{c1} - I_{c2}}{I_{c1} + I_{c2}}$ $\Delta t_{c49} = \frac{I_{c1} - I_{c2}}{I_{c1} + I_{c2}}$ $\Delta t_{c50} = \frac{I_{c1} - I_{c2}}{I_{c1} + I_{c2}}$ $\Delta t_{c51} = \frac{I_{c1} - I_{c2}}{I_{c1} + I_{c2}}$ $\Delta t_{c52} = \frac{I_{c1} - I_{c2}}{I_{c1} + I_{c2}}$ $\Delta t_{c53} = \frac{I_{c1} - I_{c2}}{I_{c1} + I_{c2}}$ $\Delta t_{c54} = \frac{I_{c1} - I_{c2}}{I_{c1} + I_{c2}}$ $\Delta t_{c55} = \frac{I_{c1} - I_{c2}}{I_{c1} + I_{c2}}$ $\Delta t_{c56} = \frac{I_{c1} - I_{c2}}{I_{c1} + I_{c2}}$ $\Delta t_{c57} = \frac{I_{c1} - I_{c2}}{I_{c1} + I_{c2}}$ $\Delta t_{c58} = \frac{I_{c1} - I_{c2}}{I_{c1} + I_{c2}}$ $\Delta t_{c59} = \frac{I_{c1} - I_{c2}}{I_{c1} + I_{c2}}$ $\Delta t_{c60} = \frac{I_{c1} - I_{c2}}{I_{c1} + I_{c2}}$ $\Delta t_{c61} = \frac{I_{c1} - I_{c2}}{I_{c1} + I_{c2}}$ $\Delta t_{c62} = \frac{I_{c1} - I_{c2}}{I_{c1} + I_{c2}}$ $\Delta t_{c63} = \frac{I_{c1} - I_{c2}}{I_{c1} + I_{c2}}$ $\Delta t_{c64} = \frac{I_{c1} - I_{c2}}{I_{c1} + I_{c2}}$ $\Delta t_{c65} = \frac{I_{c1} - I_{c2}}{I_{c1} + I_{c2}}$ $\Delta t_{c66} = \frac{I_{c1} - I_{c2}}{I_{c1} + I_{c2}}$ $\Delta t_{c67} = \frac{I_{c1} - I_{c2}}{I_{c1} + I_{c2}}$ $\Delta t_{c68} = \frac{I_{c1} - I_{c2}}{I_{c1} + I_{c2}}$ $\Delta t_{c69} = \frac{I_{c1} - I_{c2}}{I_{c1} + I_{c2}}$ $\Delta t_{c70} = \frac{I_{c1} - I_{c2}}{I_{c1} + I_{c2}}$ $\Delta t_{c71} = \frac{I_{c1} - I_{c2}}{I_{c1} + I_{c2}}$ $\Delta t_{c72} = \frac{I_{c1} - I_{c2}}{I_{c1} + I_{c2}}$ $\Delta t_{c73} = \frac{I_{c1} - I_{c2}}{I_{c1} + I_{c2}}$ $\Delta t_{c74} = \frac{I_{c1} - I_{c2}}{I_{c1} + I_{c2}}$ $\Delta t_{c75} = \frac{I_{c1} - I_{c2}}{I_{c1} + I_{c2}}$ $\Delta t_{c76} = \frac{I_{c1} - I_{c2}}{I_{c1} + I_{c2}}$ $\Delta t_{c77} = \frac{I_{c1} - I_{c2}}{I_{c1} + I_{c2}}$ $\Delta t_{c78} = \frac{I_{c1} - I_{c2}}{I_{c1} + I_{c2}}$ $\Delta t_{c79} = \frac{I_{c1} - I_{c2}}{I_{c1} + I_{c2}}$ $\Delta t_{c80} = \frac{I_{c1} - I_{c2}}{I_{c1} + I_{c2}}$ $\Delta t_{c81} = \frac{I_{c1} - I_{c2}}{I_{c1} + I_{c2}}$ $\Delta t_{c82} = \frac{I_{c1} - I_{c2}}{I_{c1} + I_{c2}}$ $\Delta t_{c83} = \frac{I_{c1} - I_{c2}}{I_{c1} + I_{c2}}$ $\Delta t_{c84} = \frac{I_{c1} - I_{c2}}{I_{c1} + I_{c2}}$ $\Delta t_{c85} = \frac{I_{c1} - I_{c2}}{I_{c1} + I_{c2}}$ $\Delta t_{c86} = \frac{I_{c1} - I_{c2}}{I_{c1} + I_{c2}}$ $\Delta t_{c87} = \frac{I_{c1} - I_{c2}}{I_{c1} + I_{c2}}$ $\Delta t_{c88} = \frac{I_{c1} - I_{c2}}{I_{c1} + I_{c2}}$ $\Delta t_{c89} = \frac{I_{c1} - I_{c2}}{I_{c1} + I_{c2}}$ $\Delta t_{c90} = \frac{I_{c1} - I_{c2}}{I_{c1} + I_{c2}}$ $\Delta t_{c91} = \frac{I_{c1} - I_{c2}}{I_{c1} + I_{c2}}$ $\Delta t_{c92} = \frac{I_{c1} - I_{c2}}{I_{c1} + I_{c2}}$ $\Delta t_{c93} = \frac{I_{c1} - I_{c2}}{I_{c1} + I_{c2}}$ $\Delta t_{c94} = \frac{I_{c1} - I_{c2}}{I_{c1} + I_{c2}}$ $\Delta t_{c95} = \frac{I_{c1} - I_{c2}}{I_{c1} + I_{c2}}$ $\Delta t_{c96} = \frac{I_{c1} - I_{c2}}{I_{c1} + I_{c2}}$ $\Delta t_{c97} = \frac{I_{c1} - I_{c2}}{I_{c1} + I_{c2}}$ $\Delta t_{c98} = \frac{I_{c1} - I_{c2}}{I_{c1} + I_{c2}}$ $\Delta t_{c99} = \frac{I_{c1} - I_{c2}}{I_{c1} + I_{c2}}$ $\Delta t_{c100} = \frac{I_{c1} - I_{c2}}{I_{c1} + I_{c2}}$

Fig 5. Track candidates are linked using a matching score S_{match} , which considers confidence values, and velocities of match candidates one frame before and after the time point of interest.

Study Materials and Methods

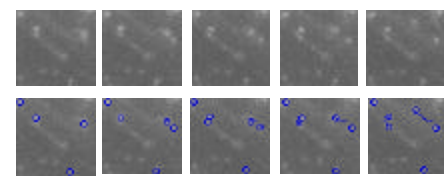


Fig 6. Four time-lapse image sets showing vesicle dynamics in pancreatic duct epithelial cells were used in the study. The figure shows a representative image sequence with study track segments overlain. Two sets of images were from an epi-fluorescence microscope, and two were from a total internal fluorescence microscopy microscope. The vesicles were labeled with FM-143. Each movie contained 85 frames captured at one frame per second. The pixel size is 0.11 μm by 0.11 μm .

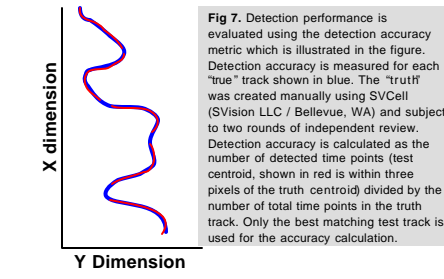


Fig 7. Detection performance is evaluated using the detection accuracy metric which is illustrated in the figure. Detection accuracy is measured for each "true" track shown in blue. The "truth" was created manually using SVCell (SVision LLC / Bellevue, WA) and subject to two rounds of independent review. Detection accuracy is calculated as the number of detected time points (test centroid, shown in red) is within three pixels of the truth centroid divided by the number of total time points in the truth track. Only the best matching test track is used for the accuracy calculation.

Results

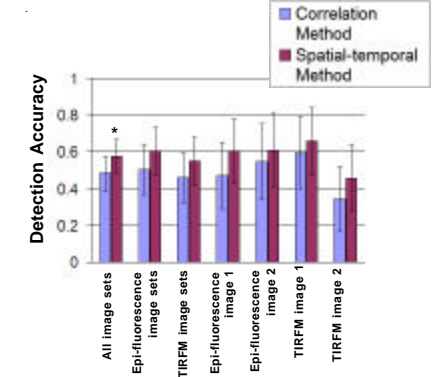


Fig 8. Study results show that the spatial temporal method of candidate matching is consistently and significantly better than the correlation method for these image sets. * Indicates a significant difference at the 90% confidence level (p value < 0.1). Values show the mean detection error comparing the spatial-temporal method and correlation method. Error bars show the 90% confidence interval.

Future Efforts

- We will continue to compare these methods using different types of experimental images from additional assays
- We will further incorporate tracking information to improve the detection

Acknowledgments

This research was supported in part by grant no. 1R43GM07774-01 from the NIGMS